



DEPARTMENT OF COMMUNITY SERVICES AND HEALTH

Australian Radiation Laboratory



**Estimates of the Radiation Dose from Phospho-gypsum
Plaster-board if Used in Domestic Buildings**

by

Richard S. O'Brien, John R. Peggie and Ian S. Leith

ARL/TR098
ISSN 0157-1400
FEBRUARY 1991

LOWER PLENTY ROAD
YALLAMBIE VICTORIA 3085
TELEPHONE: 433 2211

AUSTRALIAN RADIATION LABORATORY

Estimates of the Radiation Dose from Phospho-gypsum
Plaster-board if Used in Domestic Buildings

by

Richard S. O'Brien, John R. Peggie
and Ian S. Leith

ARL/TR098
ISSN 0157-1400
FEBRUARY 1991

LOWER PLENTY ROAD
YALLAMBIE VICTORIA 3085
TELEPHONE: 433 2211

ABSTRACT

This report presents the results of a study carried out to estimate the annual effective dose equivalent contribution from phospho-gypsum plaster-board if it were used as an internal lining in buildings. The study considered four sources of radiation exposure that would arise in such use, viz. inhalation of ^{222}Rn and its daughters, inhalation of phospho-gypsum dust and exposure to beta and gamma radiation. Measurements of the ^{226}Ra content and ^{222}Rn exhalation rate were made for a number of samples of phospho-gypsum plaster-board, and the behaviour of ^{222}Rn and its daughters in a typical building was modelled. The results of the study suggest that, for building ventilation rates greater than approximately 0.5 air changes per hour, the contribution to the total annual effective dose equivalent from inhalation of radon (^{222}Rn) and its daughters (^{218}Po , ^{214}Pb , ^{214}Bi and ^{214}Po) exhaled from the phospho-gypsum plaster-board should be well below the recommended limit of 1 milli-Sievert for members of the public. The results also suggest that this contribution will be reduced if the surface of the plaster-board is coated with paint or wallpaper or if the very fine particles are removed from the phospho-gypsum during manufacture of the plaster-board. An estimate of the potential hazard arising from dust generation during the installation of the phospho-gypsum plaster-board indicates that the annual effective dose equivalent resulting from dust inhalation is also likely to be well below the recommended limit for members of the public provided reasonable work practices are observed. An estimate of the contributions to the annual effective dose equivalent due to exposure to gamma and beta radiation from the phospho-gypsum plaster-board indicates that these contributions are also well below the recommended limit for members of the public. The total annual effective dose equivalent from all these sources should be less than 0.6 milli-Sieverts, provided reasonable work practices are observed during installation of the phospho-gypsum plaster-board and the ventilation rate is kept above approximately 0.5 air changes per hour.

INTRODUCTION

Phospho-gypsum is a by-product of the processing of phosphate fertilisers and is used in several countries as a substitute for natural gypsum in the manufacture of cement, wall board and plaster (UNSCEAR 1988). Phospho-gypsum generally contains low concentrations of ^{40}K and ^{232}Th , but may contain concentrations of radionuclides of the ^{238}U series which are 5-50 times higher than in normal soil (UNSCEAR 1988), or in gypsum plaster-board (Beretka et al 1985). Clearly, the use of this material in buildings would constitute an additional source of radiation exposure to workers and members of the public. Therefore this work has been carried out in response to a request from CSIRO Division of Building Construction, and Engineering to estimate the likely radiation doses should phospho-gypsum plaster-board be used as an internal lining in Australian homes.

Several samples of phospho-gypsum plaster-board^a of different densities were provided for testing. Most of these samples had no special surface or preparatory treatment; some were surfaced on one side with wall-paper, paint or cardboard, and two were prepared by sieving the phospho-gypsum through a special mesh. A list of the samples, showing the density, surface treatment and any special preparation, is shown in Table 1.

This study covered all radiation exposure pathways that may result from the use of phospho-gypsum plaster-boards of the type supplied for testing. The study encompassed

- 1) measurements of the ^{226}Ra content of each sample,
- 2) measurements of the radon (^{222}Rn) exhalation rate from each sample,
- 3) numerical simulation of radon and radon daughter concentrations over a range of ventilation rates for a room with walls, floor and ceiling lined with the material being tested, and estimates of the possible radiation dose to the lungs of people living or working in buildings using this material as an internal lining,
- 4) estimates of the upper limit for the dose resulting from the inhalation of radioactive dust by workmen during the installation of the plaster-board in a building,
- 5) estimates of the upper limit for the dose resulting from exposure to gamma-radiation from the plaster-board,

^aHereafter the use of the word 'plaster-board' implies 'phospho-gypsum plaster-board' unless specifically stated otherwise

- 6) estimates of the upper limit for the dose resulting from exposure to beta-radiation from the plaster-board.

MEASUREMENTS OF ^{226}Ra CONTENT

Measurements of the ^{226}Ra content of the plaster-board samples were made by gamma-ray spectrometry. This allows a crude cross-check to be made on the exhalation rate measurements and also allows estimates of possible external dose rates to be made.

Circular discs were cut from each plaster-board sheet, weighed, and placed in a Petri dish, which was sealed twice using "Silastic". A portion of one sheet (labelled S21) was crushed and three samples for measurement were produced from the resultant powder/fibre mixture: the first sample (labelled S21 powder) consisted of a Petri dish filled with the loose material, while the other two (labelled S21-ResA and S21-ResB) consisted of the loose material mixed with silica and epoxy resin. These two latter samples were similar to the samples used to determine the efficiency of detection of the equipment used for the measurements, and were used for quality control. The sample labelled S28 was a sheet of normal (non phospho-gypsum) plaster-board, and was included for comparison purposes.

The samples were assayed by gamma-ray spectrometry using Ge detectors to determine the content of ^{226}Ra . Most of the measurements were made with two Ge detectors labelled "REGeB" and "portable". The latter is a thin germanium detector with a large surface area, especially suited to measurement of gamma rays of low energy. It also has low sensitivity to gamma rays of high energy. A single measurement was made using the Ge detector labelled "LEGe".

The method of assessment of the ^{226}Ra content consisted of sealing the sample to prevent the escape of ^{222}Rn , waiting for 10 half-lives of ^{222}Rn (about 38 days) to allow the ^{222}Rn to reach secular equilibrium with the ^{226}Ra , then measuring the nett peak counts for the gamma ray at 186 keV from ^{226}Ra and the gamma rays at 295, 352, 609, 1120 and 1764 keV from the daughters of ^{222}Rn . Because the 609 keV and higher energy peaks are not efficiently measured by the "portable" detector, they are excluded from assessment when

this detector is used and, instead, a gamma ray of low abundance at 241 keV is included.

The measurements on the samples were begun before the 38 days had elapsed, to check the degree of equilibrium. Repeat measurements were made of some samples to check for any errors introduced because of this.

The results of all these measurements are given in Table 2. Sources of uncertainty for the radon daughter method include counting uncertainties, calibration uncertainties, weighing uncertainties, uncertainties resulting from the use of the peak search program and uncertainties resulting from the fact that the geometry of the samples was not the same as that used for calibrating the equipment. The measurements on the two samples S21-ResA and S22-ResB indicate that the uncertainty due to geometry and self-absorption within the samples is approximately 10%. The counting uncertainties were found to be 1-1.5% for all samples. In the absence of definitive estimates of the other types of uncertainty we have assumed an overall uncertainty of 20% for the results obtained using the radon daughter method.

The results show that the specific activity of ^{226}Ra determined from measurements of the 186 keV gamma ray is considerably higher than that determined from the radon daughter gamma rays. The 186 keV gamma ray peak is produced by a very abundant gamma ray (53%) from ^{235}U and a low abundance gamma ray (3.28%) from ^{226}Ra , so a correction for this interference is necessary. The true correction is a moderate one, as the natural abundance of ^{226}Ra is far greater than that of ^{235}U . All these corrections have been made, resulting in two distinct values for the specific activity of ^{226}Ra , that directly from the ^{226}Ra (from the 186 keV gamma ray) being in general about 25% to 30% higher than that from the daughters of ^{222}Rn . As the uncertainty of the corrected value from the 186 keV gamma ray peak is estimated to be about 28% (1 sigma), there is no significant difference between the two sets of values, although a systematic difference obviously exists.

MEASUREMENTS OF RADON EXHALATION RATEEstimates of expected exhalation rates

The radon exhalation rate at the surface of a slab of material containing radioactivity is defined to be the flux of radon (activity) out of the surface and is measured in units of $\text{Bq m}^{-2} \text{ s}^{-1}$ or $\text{Bq m}^{-2} \text{ h}^{-1}$. The formulae used for the exhalation rate of a thin slab of material are:

where one surface is considered impermeable to radon (see Appendix)

$$J = ER\rho\lambda L \cdot \tanh[H/L] \quad \dots(A)$$

and, where both surfaces are equally permeable

$$J = ER\rho\lambda L \cdot \tanh[H/(2L)] \quad \dots(B)$$

where E is the dimensionless emanation coefficient for the plaster-board, i.e. the fraction of ^{222}Rn atoms produced that move into the pore space in the plaster-board (see also Appendix),

R (Bq kg^{-1}) is the specific activity of ^{226}Ra in the plaster-board,

ρ (kg m^{-3}) is the mass density of the plaster-board,

λ ($2.1 \times 10^{-6} \text{ s}^{-1}$) is the decay constant for radon,

H (m) is the thickness of the plaster-board sample,

$L = (D/\lambda)^{0.5}$ (m) is the effective diffusion length of the plaster-board,

$D = \gamma D_m$,

γ is the tortuosity of the plaster-board, and

D_m ($\text{m}^2 \text{ s}^{-1}$) is the molecular diffusion coefficient for radon in air.

It is important to note that these results only apply when the radon concentration at the surface(s) of the slab is zero.

The results of the measurements of ^{226}Ra , together with some reasonable assumptions about other properties of the samples such as porosity, enable rough estimates of the expected radon exhalation rates to be made as follows. We assume (following Hart et al, 1986) that $E \approx 0.2$, $D_m \approx 1.2 \times 10^{-5} \text{ m}^2 \text{ s}^{-1}$, and $\gamma = 0.7$, and adopt values for R, ρ and H (based on the data given in Tables 1 and 2) of 400 Bq kg^{-1} , 1100 kg m^{-3} , and 0.01 m respectively. Substituting these values into equation (A) gives an estimate for the exhalation rate of the plaster-board of approximately $0.0018 \text{ Bq m}^{-2} \text{ s}^{-1}$ ($6.7 \text{ Bq m}^{-2} \text{ h}^{-1}$), while

equation (B) gives an estimate of approximately $0.0009 \text{ Bq m}^{-2} \text{ s}^{-1}$ ($3.3 \text{ Bq m}^{-2} \text{ h}^{-1}$). Measurements have shown that a typical value for the environmental exhalation rate is approximately $0.02 \text{ Bq m}^{-2} \text{ s}^{-1}$ ($72 \text{ Bq m}^{-2} \text{ h}^{-1}$) (UNSCEAR 1988).

Exploratory measurements

Direct measurements of the exhalation rate of radon (^{222}Rn) from the plaster-board sheets were made using methods based on the charcoal canister method (Countess, 1975 and 1976). Four of the sheets were chosen for this study; two of the sheets with no surface treatment were used, together with one of the sheets with cardboard covering and one of the sheets with wall-paper covering. The first set of measurements was made using charcoal canisters with a collection area of 0.00385 m^2 . No attempt was made to seal the edges of the canister to the surface of the plaster-board sheets. Three cups were placed on each sheet. An additional group of cups were used as controls; these were placed on surfaces which had previously been measured or which were chosen because it was thought that their exhalation rates would be extremely low (e.g. the top of a wooden desk and the top of a steel filing cabinet were used).

The results of these measurements (shown in Table 3a) are consistent with the estimates given in the previous paragraph, but display considerable variability for each sheet that was tested. There are several possible explanations for this. Because the samples were thin (0.01 m thick sheets), it is possible that the presence of the charcoal might cause a reduction in the radon concentration near the surface of the plaster-board sheet. This in turn could cause a change in the concentration gradient of the radon and hence a change in the radon flux through the surface of the sheet. In addition, the exhalation rates of the plaster-board sheets were considerably lower than normal environmental exhalation rates; at these much lower exhalation rates the canister might not be able to collect enough radon to give reasonable counting statistics, and any perturbing effect such as that just described would be enhanced by the small collecting area of the canister. It is also possible that the canister might take up radon from the air above the opposite surface of the plaster-board sheet; in this case radon passing through the sheet would be adsorbed by the charcoal. Another possibility is that the radon collected in the canister comes from a much larger volume of the plaster-board sheet than that defined by the area of the canister, due to horizontal diffusion in the sheet because of the effect of the charcoal on the

concentration gradient of radon in the sheet. Still another possibility is that the variability in the results might be due to inhomogeneities in the distribution of ^{226}Ra in the plaster-board sheets. In addition, because the canister is not sealed to the plaster-board sheet, radon in room air may diffuse into the canister and also be adsorbed by the charcoal.

These measurements were repeated using the same canisters but sealing them to the plaster-board sheets with "Blue Tack" and "Apiezon" vacuum sealant as shown in Fig. 1. The results are shown in Tables 3b and 3c respectively. In both cases the results still show considerable variability for the individual sheets, but this variability is more pronounced for the measurements made with the Apiezon sealant.

Improved methods of measuring exhalation rate

In an attempt to improve on these exploratory methods and reduce the perturbing effect of any pressure gradient set up across the surfaces of the plaster-board sheets by the adsorbing action of the charcoal, two methods were used.

In the first method two pieces of plaster-board, each measuring 20 cm by 20 cm and separated from each other by about 3 cm, were placed, together with a charcoal canister, inside a sealed vessel. This method avoided the possibility that radon from the room would be collected in the charcoal canister and also avoided problems due to the possibility that the radon concentration gradient in the plaster-board sheets could be distorted by the adsorption action of a charcoal canister placed on one side of the sheet as in the series of exploratory measurements. Two pieces of plaster-board were used to increase the amount of radon collected. For this series of measurements a control consisting of a canister placed by itself in a similar sealed vessel was used. The results of these measurements for the untreated samples are shown in Table 4a, while the results for the treated samples are shown in Table 4b. These results show that the variability using this method is very much smaller than that shown in Tables 3a, 3b, and 3c, and that the measurements for individual sheets of plaster-board are repeatable to within the estimated accuracy of the measurements.

In the second method a primary collecting vessel (a commercially available 'Wok' with a collecting area of 0.0638 m^2) was used. Two 'Woks',

each containing a charcoal canister to collect the exhaled radon for counting, were mounted, as shown in Fig. 2, on opposite sides of a circular sheet of plaster-board which was cut to the same dimensions as the 'Wok'. The edges of the plaster-board were carefully sealed with plastic-coated adhesive tape to prevent any leakage of radon to or from the room. The results of these measurements are shown in Tables 5a (untreated samples) and 5b (treated samples). These results also show very much smaller variability than that obtained in the exploratory series of measurements and are repeatable from one measurement to another for the individual sheets.

The results in Tables 4a and 5a for the untreated samples are consistent with each other to within the accuracy of the measurements in nearly all cases.

NUMERICAL SIMULATION OF THE BEHAVIOUR OF RADON DAUGHTERS

A numerical model has been used to simulate the time-varying behaviour of radon and its daughters inside a 'typical' house and to estimate the effective dose equivalent to the lung from the radon daughters. This type of model was first developed by Jacobi (1972). The model includes the effects of ventilation, attachment of radon daughters to aerosol particles and deposition of radon daughters onto walls and other surfaces. The effects of radon leakage through floors have not been included.

The starting point for any model of this type is to write down the general mass conservation equation for the i -th species in a fluid mixture, namely

$$\frac{\partial N_i}{\partial t} = \nabla \cdot (D_i \nabla N_i - \underline{u} N_i) + P_i - L_i \quad \dots (1)$$

where \underline{u} is the bulk velocity of the fluid in the volume being considered,
 N_i is the number density of the i -th species,
 D_i is the diffusion coefficient of the i -th species,
 P_i is the rate of production of the i -th species by processes other than those associated with the motion of the fluid,
 L_i is the rate of loss of the i -th species by processes not associated with the motion of the fluid,
 ∇ is the vector gradient operator.

When radon decays its radioactive daughter products readily become attached to any aerosol or dust particles in the air and can also plate out onto solid surfaces. The relationship between the various radionuclides in the radon decay scheme is shown in Fig. 3, which also shows the sources, sinks and transfer processes for each radionuclide.

The equations for the time variation of the different radionuclides are most easily derived by integrating the equation of mass conservation for each radionuclide over the volume of the room or house being considered and making the assumption that all the radionuclides are uniformly mixed throughout the volume being considered. These equations are most easily written in terms of the number densities. However, the measurements of radon and its daughters are made in terms of activity concentrations. In these units the equations are

$$\frac{dC_1}{dt} = E(S_e/V) + fC_1' - fC_1 - \lambda_1 C_1 \quad \dots(2)$$

$$\frac{dU_2}{dt} = fU_2' - fU_2 + \lambda_2 C_1 - \lambda_2 U_2 - a_2 N_a U_2 - w_{u2}(S_w/V)U_2 \quad \dots(3)$$

$$\frac{dA_2}{dt} = fA_2' - fA_2 + a_2 N_a U_2 - \lambda_2 A_2 - w_{a2}(S_w/V)A_2 \quad \dots(4)$$

$$\frac{dU_3}{dt} = fU_3' - fU_3 + p\lambda_3 A_2 + \lambda_3 U_2 - \lambda_3 U_3 - a_3 N_a U_3 - w_{u3}(S_w/V)U_3 \quad \dots(5)$$

$$\frac{dA_3}{dt} = fA_3' - fA_3 + (1 - p)\lambda_3 A_2 + a_3 N_a U_3 - \lambda_3 A_3 - w_{a3}(S_w/V)A_3 \quad \dots(6)$$

$$\frac{dU_4}{dt} = fU_4' - fU_4 + \lambda_4 U_3 - \lambda_4 U_4 - a_4 N_a U_4 - w_{u4}(S_w/V)U_4 \quad \dots(7)$$

$$\frac{dA_4}{dt} = fA_4' - fA_4 + \lambda_4 A_3 + a_4 N_a U_4 - \lambda_4 A_4 - w_{a4}(S_w/V)A_4 \quad \dots(8)$$

where C_1 (Bq m^{-3}) is the indoor activity concentration of ^{222}Rn ,

E ($\text{Bq m}^{-2} \text{s}^{-1}$) is the exhalation rate of ^{222}Rn ,

U_i (Bq m^{-3}) is the indoor activity concentration of the i -th unattached species,

A_i (Bq m^{-3}) is the indoor activity concentration of the i -th attached species,

N_a (particles m^{-3}) is the concentration of aerosols,

V (m^3) is the volume of the house,

$f = \frac{1}{V} \frac{dV}{dt}$ (air changes s^{-1}) is the ventilation rate,

S_e (m^2) is the area of the surfaces from which radon can be exhaled,
 S_w (m^2) is the area of the surfaces on which radon daughters can be deposited,

λ_i (s^{-1}) is the decay constant for the i -th radioactive species,

a_{ui} (m^3) is the attachment coefficient for the i -th unattached species,

w_{ui} ($m s^{-1}$) is the deposition velocity for the i -th unattached species,

w_{ai} ($m s^{-1}$) is the deposition velocity for the i -th attached species,

p is the probability of a ^{214}Pb atom becoming detached by recoil when it decays from (attached) ^{218}Po (Jacobi, 1972; Raabe, 1969),

subscript values $i = 2, 3, 4$ refer to ^{218}Po , ^{214}Pb , ^{214}Bi respectively, and primed quantities denote the corresponding outdoor concentrations.

These equations were incorporated into a computer program that was used with the FORSIM VI package (Carver et al 1979) to estimate the annual dose to the lung received by people occupying buildings in which the phospho-gypsum plaster-board is used as an internal lining.

The deposition velocities for the attached radon daughters are assumed to be the same for each species because the atomic weights for the different atoms are similar. The same assumption applies to the deposition velocities for the unattached radon daughters. Values presented by several authors for these quantities are shown in Table 6. Jacobi (1972) quotes a typical aerosol concentration for the lower atmosphere of 10^{10} particles m^{-3} ; in the absence of other data we have used this value in all calculations.

CALCULATION OF THE DOSE TO THE LUNG

Inhalation of radon and radon daughters

The dose to the lung from exposure to radon daughters in the typical house discussed in this report was calculated using the formula (ICRP, 1987)

$$H_E = 1.017 \times 10^{-5} \tau_{ih} \bar{c}_{ih} + 1.067 \times 10^{-5} \tau_{ie} \bar{c}_{ie} + 1.4 \times 10^{-5} \tau_o \bar{c}_o \quad \dots(9)$$

where subscript ih refers to indoors, at home

subscript ie refers to indoors, elsewhere

subscript o refers to outdoors,

τ is the exposure time

and \bar{c} is the equilibrium equivalent concentration of radon, given by (ICRP, 1986)

$$\bar{c} = 0.105[{}^{218}\text{Po}] + 0.516[{}^{214}\text{Pb}] + 0.379[{}^{214}\text{Bi}] \quad \dots(10)$$

where [] denotes the activity concentration (in Bq m⁻³) of the relevant radionuclide.

The occupancy times for the ICRP reference model (ICRP 1987) are

$$\begin{aligned} \tau_{ih} &= 6000 \text{ h y}^{-1} \\ \tau_{ie} &= 1500 \text{ h y}^{-1} \\ \tau_o &= 1000 \text{ h y}^{-1}. \end{aligned}$$

The computer program was first tested with the outdoor radon and radon daughter concentrations held constant, integrating until the solution reached a steady state and then comparing this solution with that obtained algebraically by setting the left hand sides of equations (2) through (8) to zero and solving the resulting set of equations. The two solutions were identical to within the accuracy of the calculations. This demonstrated that the algorithm used in the model for integrating the set of time-dependent differential equations (2) to (8) was working correctly.

The next series of tests was carried out to see if the model correctly predicted values of those quantities that can be directly measured. The two most important of these are the equilibrium factor and the unattached fraction of ²²²Rn daughters.

The equilibrium factor is defined as

$$e_p = \bar{c}/c \quad \dots(11)$$

where \bar{c} is the equilibrium equivalent concentration of radon (equation (10)) and c is the actual radon concentration.

The unattached fraction of radon daughters can be calculated from

$$f_p = \bar{c}(\text{unattached})/(\bar{c}(\text{attached}) + \bar{c}(\text{unattached})) \quad \dots(12)$$

where the arguments 'attached' and 'unattached' refer to those radon daughters attached or not attached to aerosol particles. Testing the model using the values of Jacobi from Table 6 for the deposition velocities, attachment coefficient and aerosol concentration gave values for the equilibrium factor and unattached fraction (at a ventilation rate of 0.55 air changes per hour) of 0.192 and 0.086 respectively. Knutson (1988) gave values of 0.37 and 0.065 for the equilibrium factor and unattached fraction, based on the results of measurements by several workers. To obtain Knutson's values for the equilibrium factor and unattached fraction, it was found necessary to use much lower values in our model for the deposition velocities than those used by Jacobi (Table 6), for both the unattached and attached fractions of radon daughters. It was also found necessary to use a slightly higher value for the attachment coefficient than that used by Jacobi.

The values listed against Knutson in Table 6 were those used to match the values for equilibrium factor and unattached fraction of 0.37 and 0.065 mentioned above. Knutson matched results from a similar model to the results of experiments by George et al (1983) and concluded (Knutson et al 1983) that his values for the deposition velocities needed to be further reduced to fit the measured surface deposition data; the values recommended from this study are shown in the last line of Table 6. Using these values in our model reduces the amount of deposition and increases the equilibrium factor above the value quoted in the previous paragraph. This is shown in Figure 4, which compares the value of equilibrium factor calculated by our model with values measured by Rudnick et al 1983)* and Swedjemark (1983). The discrepancy between the calculated and measured values of equilibrium factor remains a problem to be resolved elsewhere. However, it should be noted that increasing the value of equilibrium factor used in the model will tend to lead to an overestimate of the dose to the lung resulting from the inhalation of radon daughters.

A series of calculations was then carried out using the occupancy times given above and allowing the ventilation rate (expressed as air changes per hour) and radon exhalation rate to vary. The size of the 'room' used for the calculations was 3m by 3m by 3m. The ratio of exhaling surface to volume (S_e/V) was set to 2 m^{-1} . In practice this value would almost certainly be too high because a typical house would consist of more than one room, the floor would probably not be lined with plaster-board, and we have made no allowance for the presence of doors or windows. The value of the ratio of the surface

area available for deposition of radon daughters to the total volume was also set to 2 m^{-1} . In practice this value could be higher due to the presence of surfaces other than walls, e.g. furniture, and also because radon daughters will plate out on doors and windows as well as walls. The calculations were made at two exhalation rates to show the effect on the total annual effective dose equivalent of changing the exhalation rate; the higher rate of $3.6 \text{ Bq m}^{-2} \text{ h}^{-1}$ represents the approximate upper limit of the results of the exhalation rate measurements.

The results of the calculations of total annual effective dose equivalent due to inhalation of radon daughters are shown in Table 7a; the results for the zero exhalation, zero ventilation case are consistent with the (outdoor) natural background values given by UNSCEAR (1988). This Table also shows the calculated values of the equilibrium factor and unattached fraction. These results include the effects of inhaling outdoor air which has been introduced to the interior of the building by ventilation; this is shown clearly at the higher ventilation rates where the effect of increasing the radon exhalation from the plaster-board has almost no effect on the total annual effective dose equivalent.

Table 7b shows the calculated net contribution of the plaster-board to the total annual dose to the lung. It can clearly be seen from these results that this model predicts that, for an exhalation rate of $3.6 \text{ Bq m}^{-2} \text{ h}^{-1}$, the contribution of the plaster-board to the total dose received in one year due to the inhalation of radon and radon daughters is approximately 0.55 milli-Sievert (mSv) at a ventilation rate of 0.5 air changes per hour, approximately 0.15 mSv at a ventilation rate of 1 air change per hour and continues to decrease as the ventilation rate increases. These values are well below the recommended limit for members of the public of 1 mSv per year (Commonwealth of Australia 1987). Since we have used values for the radon source terms which we consider to represent an upper limit, these dose calculations should also represent an upper limit for the dose received under the specified conditions.

These results can be compared with those derived using a much simpler steady state model (UNSCEAR 1988, paras. 124 and 147). When the radon concentration is converted to equilibrium equivalent concentration, the UNSCEAR model predicts (for an exhalation rate of $3.6 \text{ Bq m}^{-2} \text{ h}^{-1}$ and a ventilation rate of 1 air change per hour) an effective dose equivalent

resulting from inhalation of radon daughters caused by decay of radon exhaled from the plaster-board of 0.21 mSv per year. This is certainly consistent with the results obtained from the present model. As a further indication of the applicability of the model, Fig. 4 shows a comparison of the equilibrium factors calculated by the model with those derived by Knutson (1988) from the results of measurements (Rudnick et al (1983) and Swedjemark (1983)) as a function of ventilation rate. The model predictions compare favourably with the measured values, but the model appears to be over-predicting the equilibrium factor (and hence the dose received) at ventilation rates less than one air change per hour. The lack of experimental data for higher ventilation rates prevents our commenting on the predictions at these higher rates.

The ICRP model (ICRP 1987) uses occupancy times derived for European and North American conditions. Because of climatic differences these values may not be appropriate for Australian conditions. One would expect that the average Australian would spend a higher proportion of time outdoors than would Europeans or North Americans. Data on time use in Australia is available, but is not given in a form which is easy to convert into the quantities required for dose calculations using the ICRP approach. Because the occupancy time in Australian homes is likely to be lower than that suggested by ICRP, and because indoor radon concentrations are generally at least as high as the outdoor concentrations (unless special precautions are taken to reduce the amount of radon entering the house from outside), the doses calculated using the ICRP occupancy times should represent an upper limit for Australian conditions.

Inhalation of radioactive dust during installation of plaster-board

For this calculation, the methodology given by ICRP Publication No. 30 (1979), together with the procedures and dose assessment conversion factors given by the Dose Assessment Guideline (1989) to the Radiation Protection (Mining and Milling) Code (1987), is used. It is assumed that

- 1) the ^{226}Ra concentration in the dust is the same as that in the plaster-board,
- 2) only radionuclides from the ^{238}U decay series are present,
- 3) the dust concentration is equal to the nuisance dust limit of 10 mg m^{-3} (NHMRC, 1977),
- 4) the breathing rate is $1.2 \text{ m}^3 \text{ h}^{-1}$ (ICRP, 1979),

- 5) the exposure period is 2000 h y^{-1} (ICRP, 1979),
- 6) the specific activity for each alpha-emitting radionuclide in the ^{238}U decay series is 400 Bq kg^{-1} , and
- 7) there is no disequilibrium between the successive radionuclides in the decay series.

The calculation leads to an estimate of the annual effective dose equivalent due to the inhalation of radioactive dust from the plaster-board ranging from 0.5 mSv, for particles with an Activity Median Aerodynamic Diameter (AMAD) of $5 \mu\text{m}$, up to 1.5 mSv for particles with an AMAD of $1 \mu\text{m}$. These values represent upper limits; if the dust concentration is kept below 1 mg m^{-3} (e.g. by the use of respirators) the figures quoted above reduce to 0.05 mSv and 0.15 mSv respectively. This suggests that, provided reasonable work practices are used, the contribution to the total annual effective dose equivalent from dust inhalation should be well below the recommended limit of 1 mSv per year for members of the public.

Estimate of the annual effective dose equivalent resulting from exposure to gamma-radiation from the plaster-board

In the absence of scattering, the gamma-radiation exposure rate at a point in the centre of a spherical shell of thickness dr can be calculated using the methodology of Thomson et al (1980). Combining the measured ^{226}Ra specific activities with the values of abundances and gamma-ray exposure factors given in their Table 4.1, converting to SI units, and assuming, as before, that there is no disequilibrium caused by loss of radon, the total exposure rate for the ^{238}U decay chain is estimated. Using a value of 9.7 mSv R^{-1} for the conversion from gamma-exposure to dose in human tissue (Johns et al, 1980) leads to an estimate of the annual dose equivalent due to exposure to gamma radiation from the plaster-board in a room 3m by 3m by 3m of approximately 0.065 mSv. This assumes that the walls, floor and ceiling are lined with plaster-board sheets 1 cm thick and that there are no doors or windows, so this value should represent an upper limit; this value is also well below the recommended limit of 1 mSv for members of the public.

Estimate of the annual effective dose equivalent resulting from exposure to beta-radiation from the plaster-board

The annual limit for the dose equivalent to members of the public resulting from exposure of the skin to external radiation (alpha-radiation and beta-radiation) is 50 mSv (Commonwealth of Australia 1987). Using equation (8.149) from Fitzgerald et al (1967) and assuming that the E_2 term in that equation is zero (this gives the worst case estimate as it assumes that there is no absorption of the beta-particles within the plaster-board), and using values of maximum beta energy given by the U.S. Bureau of Radiological Health (1970) leads to an estimate of the dose equivalent due to beta-radiation at the surface of the plaster-board (assuming no disequilibrium) from the ^{238}U decay chain, for an annual exposure time of 6000 hours per year, of 3 mSv per year. This is much lower than the recommended limit of 50 mSv per year. The contribution to the effective dose equivalent resulting from exposure to beta-radiation can be found by multiplying this dose equivalent of 3 mSv per year by the recommended weighting factor of 0.06 for skin (ICRP 1979); this results in a contribution of 0.18 mSv per year for skin in direct contact with the surface of the plaster-board for the full year. It is reasonable to conclude that exposure to beta-radiation from the plaster-board is unlikely to pose a significant radiological hazard.

DISCUSSION

The results of the measurements of exhalation rates from the untreated plaster-board samples using the single sealed vessel (Table 4a) and the two 'Woks' (Table 5a) are consistent with each other and repeatable for individual sheets. The "Wok" measurements for these samples (Table 5a) also show that the exhalation rates on the two sides of the plaster-board sheet are equal within the limits of the method used. These results are also comparable with the estimates made using the theoretical formula (B) and the results of the measurements of ^{226}Ra content. Since the methods used give consistent results, and the results obtained using the single sealed vessel are repeatable to within the accuracy of the measurements, we can reasonably conclude that these two methods gave reliable estimates of the exhalation rates of the plaster-board samples.

The results of the exhalation rate measurements for the treated samples (Table 5b) show clearly that the wall-paper has little effect on the radon

exhalation rate, while the paint and cardboard significantly reduce the exhalation rate through the side of the sheet to which they are applied. These results also show that in those cases where the exhalation rate is reduced on the treated side of the sheet, the exhalation rate on the untreated side of the sheet increases.

The theory outlined in the Appendix can be extended to the case where the plaster-board sheet is coated with a covering material (e.g. cardboard). The theoretical calculation predicts that, if the covering is applied to only one surface and no change is made to the other surface, so that ^{222}Rn can pass freely through this surface (i.e. the case corresponding to formula (B) with one surface covered), the exhalation rate will be reduced on the covered side of the sheet, but will be enhanced on the untreated side. This is consistent with the results of the measurements. The theoretical calculation also predicts that if one side of the sheet is impermeable and a covering material is applied to the other side of the sheet, (the case corresponding to formula (A)) the covering material will have very little effect on the exhalation rate through that surface, unless the cover is very thick. This may be important if both surfaces of the plaster-board are treated or if the plaster-board is to be used with different wall types, e.g. brick walls, where the plaster-board is backed by a thick layer of brick so that one surface is very much less permeable than the other, or stud-framed walls, where both surfaces (if untreated) are equally permeable.

The radon exhalation rates for the samples prepared by sieving through the +300 mesh are 25-30% lower than those for the samples prepared by sieving through the -300 mesh. This is consistent with results obtained by Beretka et al (1985), who suggest that the higher exhalation rate from material with smaller particles is due to the fact that these particles seem to contain a higher concentration of radioactive nuclides.

The measured exhalation rates in the plaster-board ($2 - 3 \text{ Bq m}^{-2} \text{ h}^{-1}$) are small compared to the production rate of ^{222}Rn (approximately $30 \text{ Bq m}^{-2} \text{ h}^{-1}$); more than 90% of the radon produced in the plaster-board is trapped and decays there. It follows that when the measurements of ^{226}Ra were made on the sealed samples, the ^{222}Rn was very close to secular equilibrium with the ^{226}Ra . For this reason, we felt justified in using the ^{226}Ra values determined from measurements of the radon daughter gamma-rays in the subsequent dose estimates.

CONCLUSIONS

Radon inhalation

Using the results of the exhalation rate measurements for the untreated samples in a numerical model leads to the estimates of effective dose equivalent to the lung shown in Figure 5. These results suggest that if the plaster-board is used in buildings where the ventilation rate is maintained at levels of approximately 0.5 air changes per hour or greater, the contribution from the plaster-board to the annual effective dose equivalent for the occupants should not exceed approximately 0.54 mSv for inhalation of radon daughters. This value is well below the recommended annual limit for members of the public of 1 mSv. The results of this study also suggest that coating the surface of the plaster-board with paint or cardboard will reduce the radon exhalation rate and hence reduce the contribution to the annual effective dose equivalent resulting from the inhalation of radon daughters.

This estimate of 0.54 mSv may be compared with the results of measurements in Australian homes (Langroo et al 1990), which indicate a value of effective dose equivalent of (0.5 ± 0.5) mSv for radon daughter inhalation.

Gamma radiation

The effective dose equivalent due to exposure to gamma radiation from the plaster-board sheets is estimated to be approximately 0.065 mSv which is also well below the recommended annual limit for members of the public.

This estimate may be compared with the value of effective dose equivalent of (0.9 ± 0.1) mSv for exposure to gamma radiation measured in Australian homes (Langroo et al 1990).

Dust inhalation

The effective dose equivalent due to inhalation of dust generated during the installation of the plaster-board should also be well below the recommended annual limit of 1 mSv for members of the public, provided reasonable work practices are observed.

Beta radiation

The estimates given earlier show that beta radiation is unlikely to make any significant contribution to the total effective dose equivalent resulting from the possible use of the phospho-gypsum plaster-board.

Overall dose

The estimated total effective dose equivalent due to the possible use of the phospho-gypsum plaster-board in Australian homes is approximately 0.6 mSv, provided the ventilation rate is kept above 0.5 air changes per hour. This estimate is well below the value of (1.4 ± 0.5) mSv measured in Australian homes by Langroo et al (1990).

REFERENCES

- Batchelor, G.K. An introduction to fluid dynamics. Cambridge University Press; 1967:73-75.
- Beretka, J.; Mathew, P.J. Natural radioactivity of Australian building materials, industrial wastes and by-products. Health Physics 48:87-95; 1985.
- Carver, M.B.; Stewart, D.G.; Blair, J.M.; Selander, W.N. The FORSIM VI simulation package for the automated solution of arbitrarily defined partial and/or ordinary differential equation systems. Atomic Energy of Canada Limited, Chalk River Nuclear Laboratories; 1979.
- Cohen, B.L.; Cohen, E.S. Theory and practice of radon monitoring with charcoal adsorption. Health Physics 45:501-508; 1983.
- Commonwealth of Australia. Code of Practice on Radiation Protection in the Mining and Milling of Radioactive Ores (1987). Canberra: Australian Government Publishing Service; 1987.
- Countess, R.J. Measurement of ^{222}Rn flux with charcoal canisters. HASL-325; 1975.
- Countess, R.J. ^{222}Rn flux measurements with a charcoal canister. Health Physics 31:455-456; 1976.
- Fitzgerald, J.J.; Brownell, G.L.; Mahoney, F.J. Mathematical theory of radiation dosimetry. New York: Gordon and Breach Science Publishers, Inc.; 1967.
- George, A.C.; Knutson, E.O.; Tu, K.W. Radon daughter plateout-I: measurements. Health Physics 45:439-444; 1983.
- Green, H.S.; Leipnik, R.P. Sources of plasma physics. Wolters-Noordhoff Publishing; 1970:199-200.

- Guideline to the Radiation Protection (Mining and Milling) Code (1987). Assessment of doses and control of exposure to meet the radiation protection standards. February 1989 draft; ARL 1989.
- Hart, K.P.; Levins, D.M.; Fane, A.G. Steady-state Rn diffusion through tailings and multiple layers of covering materials. Health Physics 50:369-379; 1986.
- International Commission on Radiological Protection. Limits for intakes of radionuclides by workers. Oxford: Pergamon Press; ICRP Publication 30, Part 1; Ann. ICRP 2(3/4):1-116; 1979.
- International Commission on Radiological Protection. Radiation protection of workers in mines. Oxford: Pergamon Press; ICRP Publication 47; Ann. ICRP 16(1):1-21; 1986.
- International Commission on Radiological Protection. Lung cancer risk from indoor exposures to radon daughters. Oxford: Pergamon Press; ICRP Publication 50; Ann. ICRP 17(1):1-60; 1987.
- Jacobi, W. Activity and potential α -energy of ^{222}Rn - and ^{220}Rn -daughters in different air atmospheres. Health Physics 22:441-450; 1972.
- Johns, H.E.; Cunningham, J.R. The physics of radiology. Charles C. Thomas; 1983.
- Knutson, E.O. Modelling indoor concentrations of radon's decay products. In: Nazaroff, W.W.; Nero, A.V. Jr., eds. Radon and its decay products in indoor air. New York: John Wiley and Sons; 1988:Chapter 5.
- Knutson, E.O.; George, A.C.; Frey, J.J.; Koh, B.R. Radon daughter plateout-II: prediction model. Health Physics 45:445-452; 1983.
- Langroo, M.K.; Wise, K.N.; Duggleby, J.C.; Kotler, L.H. A nation-wide survey of ^{222}Rn and gamma radiation levels in Australian homes. Submitted to Health Physics.
- Mercer, T.T. The effect of particle size on the escape of recoiling RaB atoms from particulate surfaces. Health Physics 31:173-175; 1976.

- National Health and Medical Research Council. Report of the Eighty-fourth Session, Canberra, November 1977. Canberra: Australian Government Publishing Service; 1978.
- Porstendorfer, J.; Wicke, A.; Schraub, A. The influence of exhalation, ventilation and deposition processes upon the concentration of radon (^{222}Rn), thoron (^{220}Rn) and their decay products in room air. Health Physics 34:465-473; 1978.
- Raabe, O.G. Concerning the interactions that occur between radon decay products and aerosols. Health Physics 17:177-185; 1969.
- Rudnick, S.N.; Hinds, W.C.; Maher, E.F.; First, M.W. Effect of plateout, air motion and dust removal on radon decay product concentration in a simulated residence. Health Physics 45:463-470; 1983.
- Scott, A.G. Radon daughter deposition velocities estimated from field measurements. Health Physics 45:481-485; 1983.
- Strong, K.P.; Levins, D.M. Effect of moisture content on radon emanation from uranium ore and tailings. Health Physics 42:27-32; 1982.
- Swedjemark, G.A. The equilibrium factor F. Health Physics 45:453-462; 1983.
- Thomson, J.E.; Wilson, O.J. Calculation of gamma ray exposure rates from uranium ore bodies. Australian Radiation Laboratory Technical Report ARL/TR 014; February 1980.
- United Nations Scientific Committee on the Effects of Atomic Radiation. Sources, effects and risks of ionizing radiation. New York: United Nations; 1988.
- United States Bureau of Radiological Health. Radiological Health Handbook, (revised edition). U.S. Dept. of Health, Education and Welfare, Rockville, Md., p 112, 1970.

APPENDIX: Theoretical derivation of the expression for the exhalation rate of radon from a slab of material containing ^{226}Ra .

The differential equation governing the diffusion of radon in the pore space of a material containing ^{226}Ra can be written (Batchelor, 1967; Green et al, 1970; Hart et al, 1986) as

$$\frac{\partial(\epsilon C)}{\partial t} + \nabla \cdot (\epsilon C \underline{U} - D \nabla (\epsilon C)) = P - \lambda \epsilon C, \quad 0 \leq z \leq H \quad \dots(1)$$

where

- $P = ER\rho\lambda$ is the production rate of radon in the pore space of the material (Strong et al, 1982),
- E is the emanation coefficient of radon in the material, i.e. the fraction of radon atoms produced which move into the pore space of the material,
- R is the specific activity of ^{226}Ra in the material (Bq kg^{-1}),
- ρ is the density of the material (kg m^{-3}),
- C is the radon activity concentration (in Bq m^{-3} of air) in the pore space of the material,
- λ is the decay constant of radon ($2.1 \times 10^{-6} \text{ s}^{-1}$),
- ϵ is the porosity of the material,
- D is the effective diffusion coefficient of radon in the pore space and is given by $D = \gamma D_m$,
- γ is the tortuosity of the material,
- D_m is the molecular diffusion coefficient for radon in air ($\text{m}^2 \text{ s}^{-1}$),
- \underline{U} is the mean velocity of the air,
- ∇ denotes the vector gradient operator,
- \cdot denotes the scalar product of two vectors,
- H is the thickness of the plaster-board sample (m).

Assuming horizontal homogeneity (i.e. $\frac{\partial}{\partial x} = \frac{\partial}{\partial y} = 0$), and

integrating over x and y to remove the effect of horizontal variations in the mean vertical velocity component W , equation (1) can be written in the form

$$\frac{\partial C}{\partial t} + \frac{\partial}{\partial z} (C.W - D \cdot \frac{\partial C}{\partial z}) = P/\epsilon - \lambda C \quad \dots(2)$$

The simplest procedure is to assume that

- 1) the vertical component of velocity (W) is zero (this is equivalent to assuming that there is no pressure difference between the two sides of the slab),
- 2) steady state conditions apply.

Using these assumptions, the radon concentration in the pore space of the material can be written as

$$C(z) = \frac{P}{\lambda\epsilon} + A.\sinh(z/L) + B.\cosh(z/L) \quad \dots(3)$$

where $L = (D/\lambda)^{0.5} \quad \dots(4)$

L is the effective diffusion length of the plaster-board (m).

There are two situations of practical importance to which this solution can be applied, provided that the appropriate boundary conditions are chosen. The first is that in which one side of the slab is impermeable to radon. In this case the boundary conditions to be applied to equation (3) are

$$D\epsilon\left(\frac{dC}{dz}\right)_{z=0} = 0 \quad \dots(5)$$

i.e. the radon flux is zero through the base of the slab, and

$$C(H) = C_a \quad \dots(6)$$

where C_a is the radon concentration in the air outside the slab, and H is the thickness of the slab.

Applying (5) and (6) to (3) leads to the result

$$C(z) = \frac{P}{\lambda\epsilon} \left\{ 1 - \frac{\cosh(z/L)}{\cosh(H/L)} \right\} + C_a \cdot \frac{\cosh(z/L)}{\cosh(H/L)} \quad \dots(7)$$

The radon flux at the top surface of the slab is the exhalation rate and is given by

$$J = - D\epsilon\left(\frac{dC}{dz}\right)_{z=H} \quad \dots(8)$$

i.e. $J = (D\epsilon/L) \left(\frac{P}{\lambda\epsilon} - C_a \right) \cdot \tanh(H/L) \quad \dots(9)$

The second situation to which (3) can be applied is the case where radon can pass through both sides of the slab. In the simplest case, in which the radon concentration at the two surfaces of the slab is the same,

$$\text{i.e.} \quad C(0) = C(H) = C_a \quad \dots(10)$$

it is easy to show that equation (9) has to be replaced by

$$J(H) = -J(0) = (D\epsilon/L) \left(\frac{P}{\lambda\epsilon} - C_a \right) \tanh(H/2L) \quad \dots(11)$$

UNSCEAR (1985) give an expression for the radon exhalation rate at the ground-air interface, namely

$$J_0 = D\epsilon \left(\frac{dC}{dz} \right)_{z=0} = P(D/\lambda)^{0.5} \quad \dots(12)$$

This result is exactly the same as that obtained from equation (9) by setting $C_a = 0$ and $H = \infty$ (which corresponds to the case of an infinitely thick slab).

Comparing equations (11) and (12) suggests that, to measure J_0 accurately, we need to establish conditions in which the radon concentration at and above the exhaling surface(s) is close to zero. Cohen et al (1983) have established that the charcoal cup method of measuring radon concentration in air relies on the charcoal behaving as if it adsorbs all the radon in a given volume of air (4 litres of air per gm of charcoal). This suggests that if the collecting vessel has a volume which is considerably less than 100 litres (we used a 25 gm charge of charcoal), nearly all the radon which is exhaled from the slab will be collected in the charcoal, so the condition $C_a = 0$ will be closely approximated.

Table 1

A list of the samples used in this study, showing density, method of preparation and surface treatment

sample no.	density (g cm ⁻³)	preparation	cover.
S1	1.116		blank
S2	1.007		blank
S3	1.043		paint ^a
S4	1.041		paint ^a
S5	1.095		blank
S6	1.035		blank
S7	1.072		wallpaper ^b
S8	1.045		cardboard ^c
S9	0.975		blank
S10	1.053		blank
S11	0.987		blank
S12	1.125		blank
S13	1.122		blank
S14	1.146		blank
S16	1.057		cardboard ^c
S17	1.103		blank
S18	1.153		blank
S19	1.069		wallpaper ^b
S20	0.963		blank
S21	1.010		blank
S22	1.066	sieving (-300 mesh) ^d	blank
S24	1.045	sieving (+300 mesh) ^e	blank
S25	1.060	sieving (+300 mesh)	blank
S27	1.049	sieving (-300 mesh)	blank
S28		normal plaster-board	blank

^a paint - 2 coats of an interior/exterior oil-based undercoat, followed by two coats of flow sheen vinyl interior paint

^b wallpaper - 1 coat of wallpaper size; then covered with pre-pasted vinyl coated wallpaper

^c cardboard - stuck on with a poly-vinyl adhesive glue

^d particle sizes less than 53 μm

^e particle sizes greater than 53 μm

Table 2
Specific activity (Bq kg⁻¹) of ²²⁶Ra in samples of phospho-gypsum
 plaster-board.

Measurement			Sample Number			
No.	Method	Detector	S1	S2	S3	S4
1	186 keV	REGeB	550 ± 150	500 ± 140	600 ± 170	490 ± 140
	Daughters		420 ± 80	400 ± 80	380 ± 80	430 ± 90
	Time from sealing (d)		3	4	5	6
2	186 keV	Portable	560 ± 160	570 ± 160	620 ± 170	550 ± 150
	Daughters		430 ± 90	410 ± 80	420 ± 80	430 ± 90
	Time from sealing (d)		48	52	53	55
Measurement			Sample Number			
No.	Method	Detector	S5	S6	S7	S8
1	186 keV	REGeB	470 ± 130	560 ± 150	470 ± 130	490 ± 140
	Daughters		370 ± 70	430 ± 90	420 ± 80	350 ± 70
	Time from sealing (d)		7	25	18	10
2	186 keV	Portable	530 ± 150	580 ± 160	510 ± 140	480 ± 130
	Daughters		370 ± 70	440 ± 90	420 ± 80	360 ± 70
	Time from sealing (d)		56	57	58	60
3	186 keV	REGeB	540 ± 150	420 ± 120		
	Daughters		410 ± 80	360 ± 70		
	Time from sealing (d)		39	28		
4	186 keV	REGeB		470 ± 130		
	Daughters			360 ± 70		
	Time from sealing (d)			43		

Table 2 (cont'd)
Specific activity (Bq kg⁻¹) of ²²⁶Ra in samples of phospho-gypsum
 plaster-board.

Measurement			Sample Number			
No.	Method	Detector	S9	S10	S11	S12
1	186 keV	REGeB	520 ± 140	540 ± 150	510 ± 140	510 ± 140
	Daughters		420 ± 80	420 ± 80	420 ± 80	410 ± 80
	Time from sealing (d)		11	12	13	14
2	186 keV	Portable	540 ± 150			
	Daughters		440 ± 80			
	Time from sealing (d)		67			

Measurement			Sample Number			
No.	Method	Detector	S13	S14	S16	S17
1	186 keV	REGeB	550 ± 150	530 ± 150	550 ± 150	550 ± 150
	Daughters		440 ± 90	440 ± 90	380 ± 80	380 ± 80
	Time from sealing (d)		18	26	19	20

Measurement			Sample Number			
No.	Method	Detector	S18	S19	S21	S21(powder)
1	186 keV	REGeB	500 ± 140	510 ± 140	510 ± 140	530 ± 140
	Daughters		420 ± 80	390 ± 80	390 ± 80	420 ± 80
	Time from sealing (d)		21	27	28	38

Table 2 (cont'd)
Specific activity (Bq kg⁻¹) of ²²⁶Ra in samples of phospho-gypsum
 plaster-board.

No.	Measurement		Sample Number			
	Method	Detector	S21-ResA	S21-ResB	S22	S22-300#
1	186 keV	REGeB	590 ± 160	640 ± 180	580 ± 160	600 ± 170
	Daughters		460 ± 90	460 ± 90	410 ± 80	440 ± 90
	Time from sealing (d)		19	20	29	34
2	186 keV	Portable	580 ± 160		530 ± 150	
	Daughters		360 ± 70		410 ± 80	
	Time from sealing (d)		42		45	
3	186 keV	LEGe	440 ± 120			
	Daughters		490 ± 100			
	Time from sealing (d)		45			
No.	Measurement		Sample Number			
	Method	Detector	S24	S25	S27	S28
1	186 keV	REGeB	520 ± 150	420 ± 110	760 ± 210	not detectable
	Daughters		360 ± 70	360 ± 70	500 ± 100	8 ± 2
	Time from sealing (d)		31	32	33	
2	186 keV	Portable		490 ± 130		
	Daughters			340 ± 70		
	Time from sealing (d)			46		

Table 3a

Summary of exhalation measurements using charcoal canisters which are not sealed to the plaster-board sheets

sample no.	cover	density (g cm ⁻³)	date	sampling time (hours)	²²² Rn in cup (Bq)	exhalation rate (Bq m ⁻² h ⁻¹)
S8	card board	1.045	1-5/12	92.75	1.6 ± 0.3	6.0 ± 1.6
				92.75	0.5 ± 0.3	1.9 ± 1.2
				92.75	1.1 ± 0.3	4.2 ± 1.5
S10	blank	1.053		92.75	1.4 ± 0.3	5.4 ± 1.5
				92.75	1.0 ± 0.3	3.9 ± 1.4
				92.75	1.5 ± 0.3	6.0 ± 1.7
S18	blank	1.153		92.75	2.1 ± 0.3	8.1 ± 1.9
				92.75	1.0 ± 0.3	3.9 ± 1.4
				92.75	1.1 ± 0.3	4.4 ± 1.5
S19	wall paper	1.069		92.75	1.8 ± 0.3	7.0 ± 1.7
				92.75	1.1 ± 0.3	4.4 ± 1.5
				92.75	1.9 ± 0.4	7.4 ± 1.9
Control	wood plastic metal			92.75	1.5 ± 0.3	5.6 ± 1.5
				92.75	0.5 ± 0.3	2.1 ± 1.2
				92.75	0.7 ± 0.3	2.8 ± 1.4

Table 3b

Summary of exhalation measurements using charcoal canisters sealed to the
plaster-board sheets with "Blue Tack"

sample no.	cover	density (g cm ⁻³)	date	sampling time (hours)	²²² Rn in cup (Bq)	exhalation rate (Bq m ⁻² h ⁻¹)
S8	card board	1.045	6-11/12	116.08	0.5 ± 0.3	1.6 ± 1.0
				116.08	1.0 ± 0.3	3.3 ± 1.2
				116.08	1.4 ± 0.4	4.6 ± 1.4
S10	blank	1.053		115.87	1.5 ± 0.3	4.9 ± 1.3
				115.87	1.5 ± 0.3	5.0 ± 1.3
				115.87	1.9 ± 0.4	6.5 ± 1.6
S18	blank	1.153		116.42	1.3 ± 0.3	4.4 ± 1.2
				116.42	2.0 ± 0.3	6.7 ± 1.6
				116.42	1.9 ± 0.4	6.5 ± 1.6
S19	wall paper	1.069		115.92	0.9 ± 0.3	3.1 ± 1.1
				116.33	1.6 ± 0.3	5.5 ± 1.4
				116.42	2.1 ± 0.4	7.1 ± 1.7
Control	plastic linoleum wood			116.30	0.5 ± 0.2	1.7 ± 0.7
				116.30	0.4 ± 0.2	1.3 ± 0.7
				116.30	0.7 ± 0.2	2.2 ± 0.9

Table 3c

Summary of exhalation measurements using charcoal canisters sealed to the
plaster-board sheets with "Apiezon" vacuum sealant

sample no.	cover	density (g cm ⁻³)	date	sampling time (hours)	²²² Rn in cup (Bq)	exhalation rate (Bq m ⁻² h ⁻¹)
S8	card board	1.045	12-13/12	24.50	0.3 ± 0.3	3.8 ± 3.4
				24.50	0.4 ± 0.3	4.9 ± 3.6
				24.50	1.4 ± 0.4	16.3 ± 4.9
S10	blank	1.053		24.42	0.6 ± 0.3	7.0 ± 3.5
				24.42	0.9 ± 0.3	10.0 ± 3.9
				24.42	1.5 ± 0.4	17.3 ± 5.0
S18	blank	1.153		24.17	0.9 ± 0.3	10.5 ± 4.1
				24.17	1.0 ± 0.3	11.7 ± 4.3
S19	wall paper	1.069		24.33	1.9 ± 0.3	22.4 ± 5.3
				24.33	0.8 ± 0.3	9.4 ± 3.9
				24.33	1.9 ± 0.4	21.7 ± 5.6
Control	wood linoleum			24.08	0.1 ± 0.3	1.6 ± 3.2
				24.08	0.1 ± 0.3	0.8 ± 3.4

Table 4a

Summary of exhalation measurements for the untreated samples, using a single sealed vessel as the primary collecting vessel

sample no.	cover	density (g cm ⁻³)	date	sampling time (hours)	²²² Rn in cup (Bq)	exhalation rate (Bq m ⁻² h ⁻¹)
S1	blank	1.116	18/6/90	23.75	10.0 ± 0.8	2.7 ± 0.3
S2	blank	1.007	30/7/90	39.50	12.3 ± 0.9	2.1 ± 0.2
S5	blank	1.095	5/7/90	24.55	11.7 ± 0.9	2.9 ± 0.3
S6	blank	1.035	23/7/90	21.00	7.3 ± 0.6	2.1 ± 0.2
S9	blank	0.975	8/8/90	40.75	14.2 ± 1.1	2.3 ± 0.2
S10	blank	1.053	3/7/90	22.83	7.2 ± 0.6	2.0 ± 0.2
S11	blank	0.987	9/7/90	25.00	9.0 ± 0.7	2.3 ± 0.2
S12	blank	1.125	17/7/90	47.42	21.1 ± 1.6	3.0 ± 0.3
S13	blank	1.122	3/9/90	26.42	9.6 ± 0.8	2.8 ± 0.3
S14	blank	1.146	16/7/90	22.42	9.7 ± 0.8	2.7 ± 0.3
S17	blank	1.103	7/8/90	22.08	13.3 ± 1.0	3.7 ± 0.4
S18	blank	1.153	28/6/90	24.42	14.3 ± 1.1	3.8 ± 0.4
S20 ^a	blank	0.963	18/6/90	22.42	5.4 ± 0.5	1.8 ± 0.2
S20	blank		19/6/90	47.33	7.6 ± 0.6	2.1 ± 0.2
S21	blank	1.010	22/6/90	67.25	35.4 ± 2.6	2.5 ± 0.2
S21	blank		25/6/90	21.33	11.5 ± 0.9	2.2 ± 0.2
S28					control exceeded sample	

^a circular disc of radius 13.5 cm.

Table 4b

Summary of exhalation measurements for the treated samples, using a single sealed vessel as the primary collecting vessel

sample no.	cover	density (g cm ⁻³)	date	sampling time (hours)	²²² Rn in cup (Bq)	exhalation rate (Bq m ⁻² h ⁻¹)
S3	paint ^a	1.043	31/8/90	65.58	28.6 ± 2.1	3.1 ± 0.3
S4	paint	1.041	22/8/90	39.92	7.5 ± 0.6	2.9 ± 0.3
S7	paper ^b	1.072	17/8/90	67.42	27.3 ± 2.0	2.9 ± 0.3
S19	paper	1.069	28/8/90	48.00	28.6 ± 2.1	4.0 ± 0.4
			28/8/90	48.00	27.5 ± 2.0	3.9 ± 0.4
S8	card board ^c	1.045	20/8/90	42.83	19.3 ± 1.4	3.0 ± 0.3
S16	card board ^c	1.057	24/8/90	70.17	37.6 ± 2.7	3.9 ± 0.4
S22	blank ^d	1.066	10/7/90	70.67	26.0 ± 1.9	2.7 ± 0.3
S27	blank ^d	1.049	13/7/90	73.00	29.6 ± 2.2	3.0 ± 0.3
S24	blank ^e	1.045	2/8/90	24.58	7.2 ± 0.6	1.8 ± 0.2
S25	blank ^e	1.060	6/8/90	22.55	8.5 ± 0.7	2.3 ± 0.2

^a paint - 2 coats of an interior/exterior oil-based undercoat, followed by two coats of flow sheen vinyl interior paint

^b paper - 1 coat of wallpaper size; then covered with pre-pasted vinyl coated wallpaper

^c cardboard - stuck on with a poly-vinyl adhesive glue

^d sample prepared by sieving through a -300 mesh

^e sample prepared by sieving through a +300 mesh

Table 5a

Summary of exhalation measurements for the untreated samples, using two
"Woks" as primary collecting vessels^a

sample no.	cover	density (g cm ⁻³)	date	sampling time (hours)	²²² Rn in cup (Bq)	exhalation rate (Bq m ⁻² h ⁻¹)
S2	blank	1.007	31/7/90	40.78	5.7 ± 0.5	2.2 ± 0.2
S2			31/7/90	40.78	7.2 ± 0.6	2.7 ± 0.3
S6	blank	1.035	23/7/90	20.92	3.5 ± 0.3	2.8 ± 0.3
S6			23/7/90	20.92	3.4 ± 0.4	2.7 ± 0.3
S9	blank	0.975	8/8/90	40.75	5.2 ± 0.5	2.0 ± 0.2
S9			8/8/90	40.75	6.8 ± 0.6	2.6 ± 0.3
S17	blank	1.103	7/8/90	22.17	6.6 ± 0.5	4.3 ± 0.4
S17			7/8/90	22.17	5.9 ± 0.6	3.9 ± 0.4

^a the results for each "Wok" are shown

Table 5b

Summary of exhalation measurements for the treated samples, using two
"Woks" as primary collecting vessels^a

sample no.	cover	density (g cm ⁻³)	date	sampling time (hours)	²²² Rn in cup (Bq)	exhalation rate (Bq m ⁻² h ⁻¹)
S3 ^b	paint	1.043	31/8/90	65.58	7.2 ± 0.6	1.9 ± 0.2
S3				65.58	13.4 ± 1.0	3.4 ± 0.3
S4 ^b	paint	1.041	22/8/90	39.92	4.5 ± 0.4	1.8 ± 0.2
S4			22/8/90	39.92	10.7 ± 0.9	3.4 ± 0.3
S7 ^b	paper	1.072	17/8/90	67.22	10.8 ± 0.9	3.3 ± 0.3
S7			17/8/90	67.22	12.9 ± 1.0	3.9 ± 0.4
S19 ^b	paper	1.069	30/8/90	48.00	12.5 ± 1.0	4.1 ± 0.4
S19			30/8/90	48.00	12.9 ± 1.0	4.3 ± 0.4
S8 ^b	card	1.045	20/8/90	42.67	3.3 ± 0.3	1.2 ± 0.1
S8	board		20/8/90	42.67	11.1 ± 0.9	4.1 ± 0.4
S16 ^b	card	1.057	24/8/90	70.00	10.1 ± 0.8	2.5 ± 0.2
S16	board		24/8/90	70.00	20.1 ± 1.5	4.9 ± 0.5
S24	blank ^c	1.045	2/8/90	24.25	4.0 ± 0.4	2.4 ± 0.3
S24			2/8/90	24.25	3.6 ± 0.4	2.2 ± 0.3

^a the results for each "Wok" are shown

^b the results for the treated side are presented first

^c sample prepared by sieving through a +300 mesh

Table 6

Values of the radon daughter attachment coefficients, deposition velocities and recoil probabilities and typical aerosol concentrations as presented by the authors listed.

Source	Deposition velocity unattached (m s ⁻¹)	Deposition velocity attached (m s ⁻¹)	Attachment coefficient (m ³ s ⁻¹)	Aerosol concentration (m ⁻³)	Recoil probability
Jacobi (1972)	0.01	0.0001	1.1 x 10 ⁻¹²	1.0 x 10 ¹⁰	0.5
Porstendorfer (1978)	0.014	0.00014	1.2 x 10 ⁻¹²	1.4 x 10 ¹⁰	
Scott (1983)	0.014 - 0.05	0.00005			
Mercer (1976)					0.83
<hr/>					
Knutson (1988)	2.8x10 ⁻³	2.8x10 ⁻⁵	1.39 x 10 ⁻¹²	1.0 x 10 ¹⁰	0.83
Knutson ^a (1988)	1.8x10 ⁻⁵	1.8x10 ⁻⁷			

^a these values are included to match the surface deposition data of George et al (1983): see text.

Table 7a

Results of the calculations of the total annual effective dose equivalent to the lung (in mSv) from inhalation of radon daughters as a function of ventilation rate at exhalation rates of (a) 0.0, (b) 0.72, and (c) 3.6 ($\text{Bq m}^{-2} \text{ h}^{-1}$), for occupancy times: indoors at home $\tau_{ih} = 6000 \text{ h yr}^{-1}$, indoors elsewhere $\tau_{ie} = 1500 \text{ h yr}^{-1}$, and outdoors $\tau_o = 1000 \text{ h yr}^{-1}$.

Ventilation rate (h^{-1})	Equilibrium factor	Unattached fraction	Total annual effective dose equivalent (mSv)		
			(a)	(b)	(c)
0.0	0.88 ^a	0.038 ^a	0.44 ^b	10.62	51.33
0.25	0.73	0.046	1.29	1.54	2.53
0.50	0.62	0.053	1.17	1.28	1.71
1.00	0.48	0.067	1.01	1.05	1.21
1.50	0.39	0.081	0.90	0.92	1.01
2.00	0.33	0.095	0.83	0.84	0.90
2.50	0.28	0.11	0.78	0.79	0.83
3.00	0.25	0.12	0.74	0.74	0.77
5.00	0.17	0.17	0.64	0.65	0.66

^a not applicable to the case of zero ventilation rate and zero exhalation

^b consistent with the values expected out-of-doors for natural sources of ^{222}Rn .

Table 7b

Results of the calculations of the contribution of the plaster-board to the total annual effective dose equivalent to the lung (in mSv) from inhalation of ^{222}Rn daughters as a function of ventilation rate at exhalation rates of (a) 0.72, and (b) 3.6 ($\text{Bq m}^{-2} \text{h}^{-1}$)

Ventilation rate (air changes h^{-1})	Annual effective dose equivalent (mSv)	
	(a)	(b)
0.0	10.18	50.89
0.25	0.26	1.24
0.50	0.11	0.54
1.00	0.04	0.16
1.50	0.02	0.11
2.00	0.01	0.07
2.50	0.01	0.05
3.00	0.01	0.04
5.00	0.00	0.02

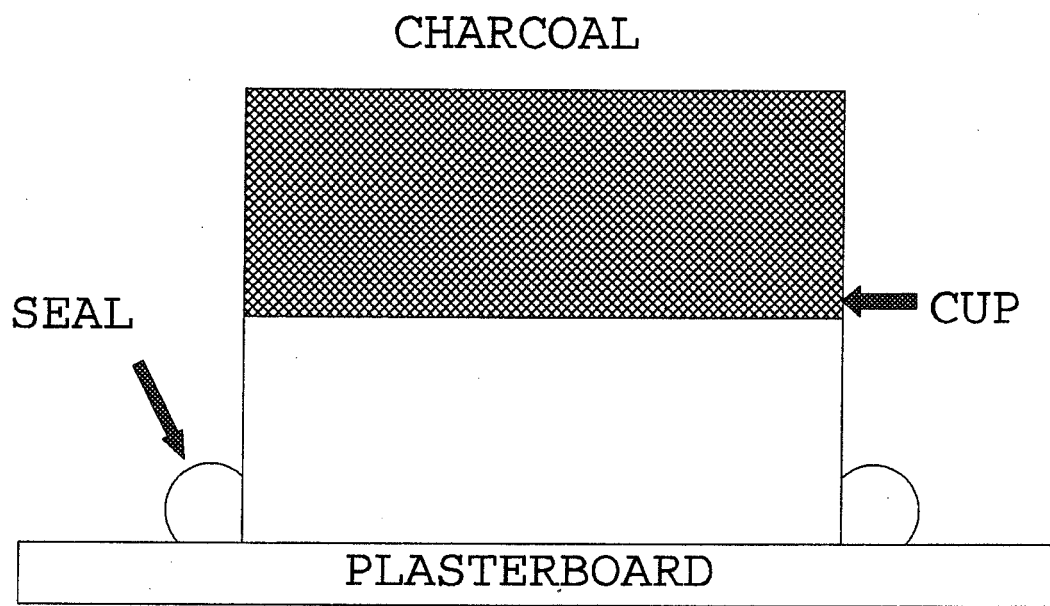


Figure 1. The charcoal cup configuration for measuring exhalation rate.

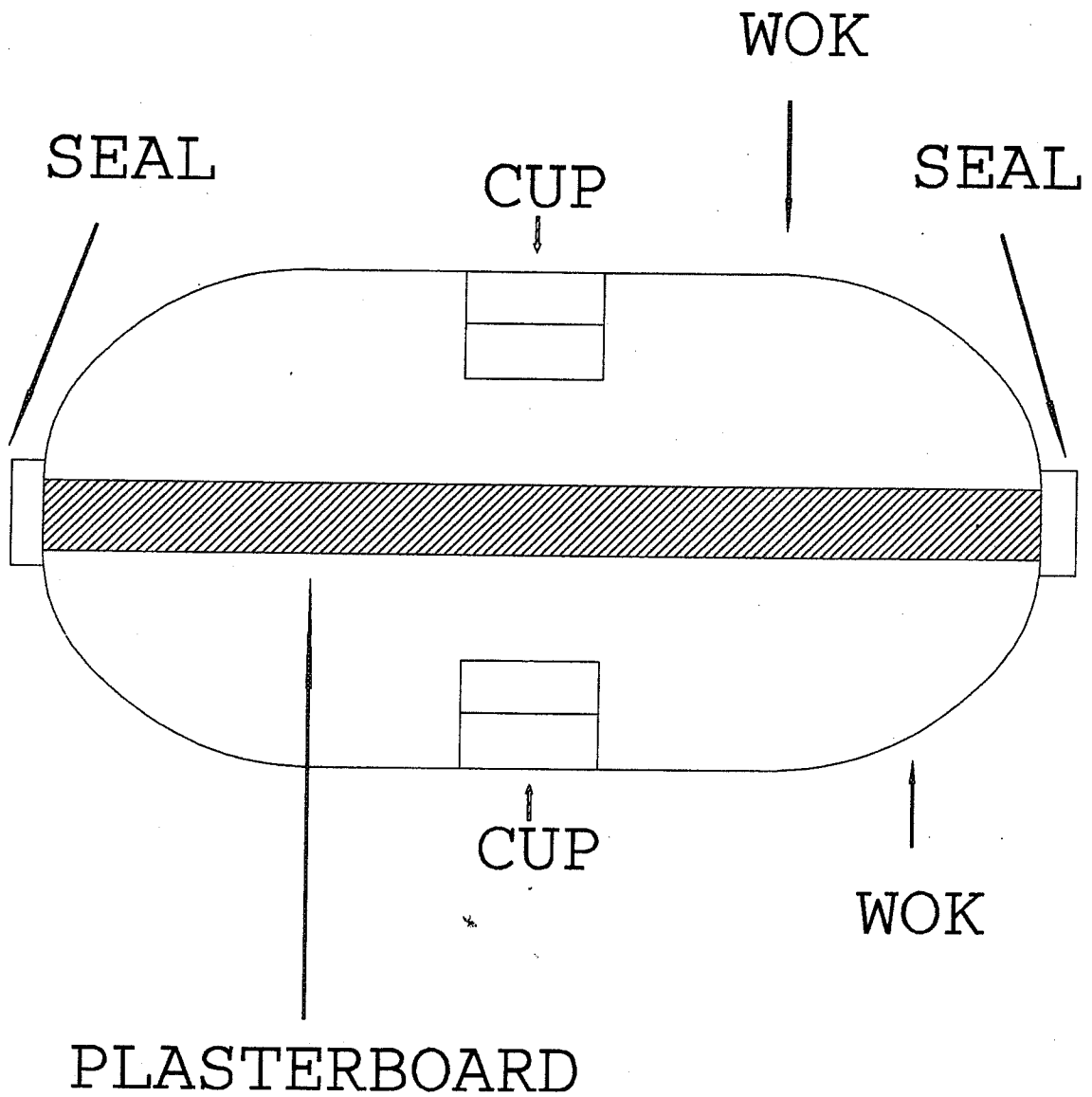


Figure 2. The double 'Wok' arrangement for measuring exhalation rate (method 2.2) in the text

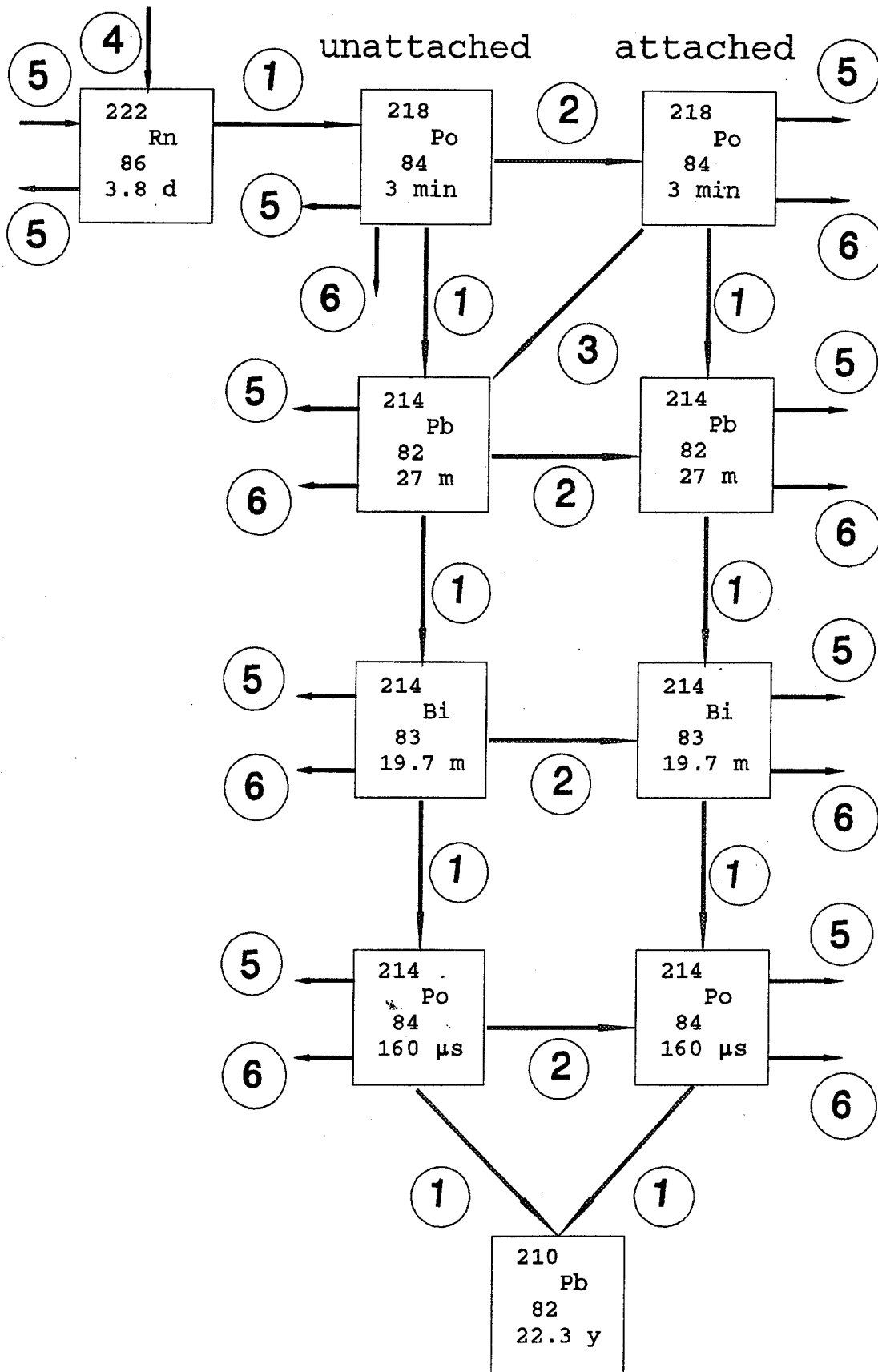


Figure 3. The ^{222}Rn decay chain showing the sources and sinks for each species included in the model, labelled as follows -: 1 = decay, 2 = attachment, 3 = recoil, 4 = exhalation, 5 = ventilation, 6 = deposition.

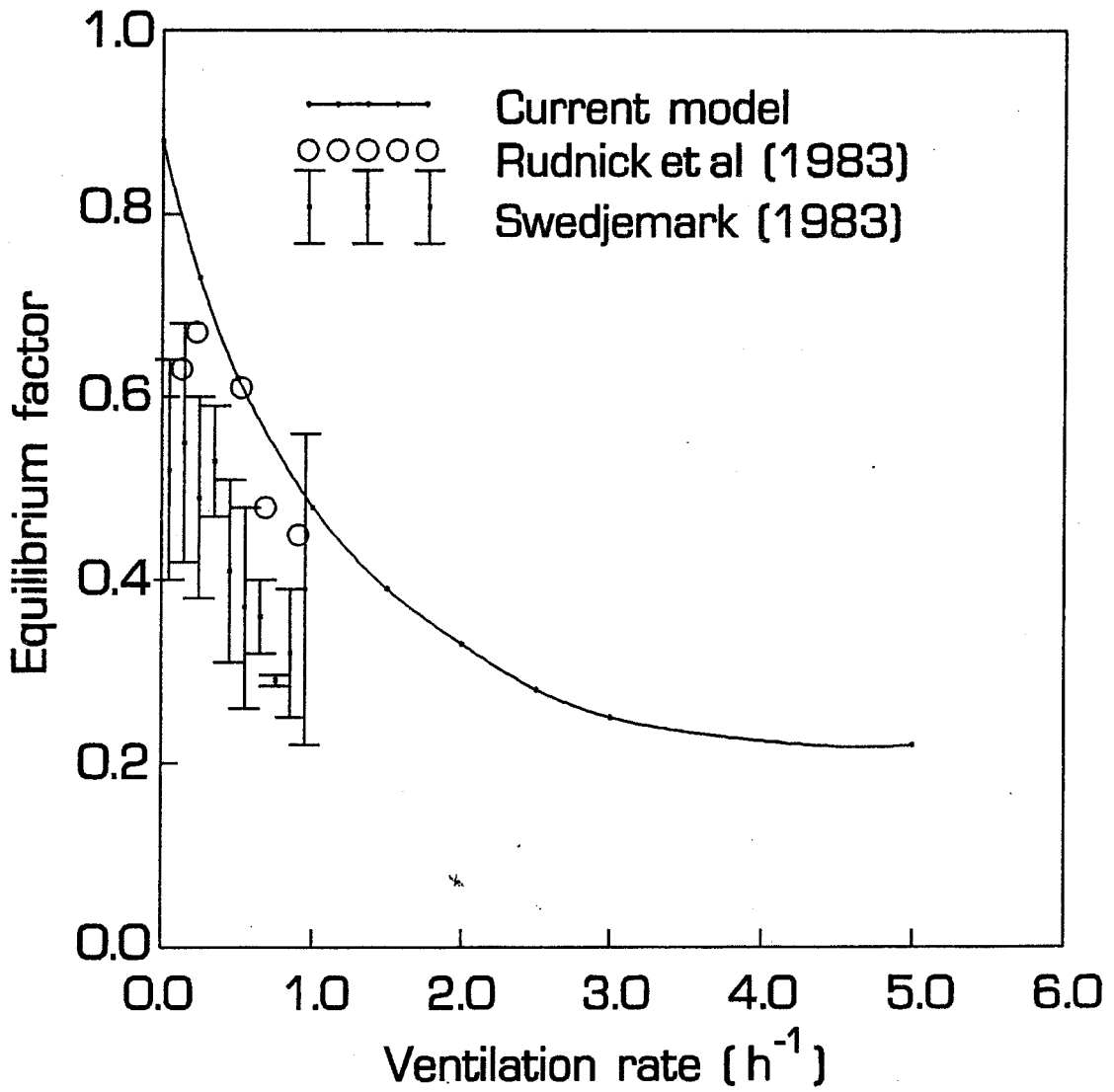


Figure 4. The F-factor calculated by the model (as a function of ventilation rate) compared with experimental data.

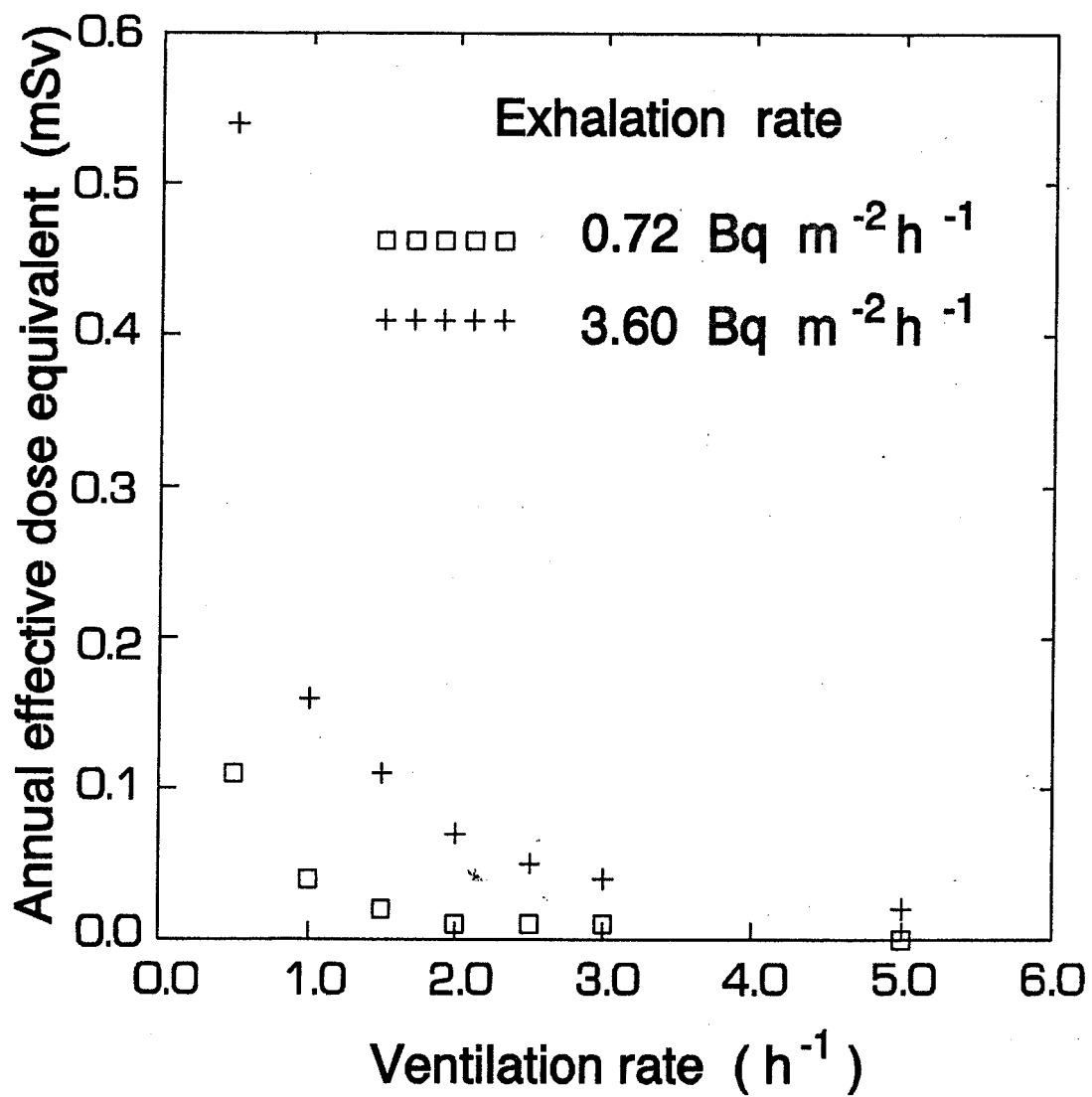


Figure 5. Annual effective dose equivalent as a function of ventilation rate and ^{222}Rn exhalation rate resulting from inhalation of ^{222}Rn daughters from the phospho-gypsum plaster-board.